Vol. 48 (2017) ACTA PHYSICA POLONICA B No 6

DIFFERENTIAL $t\bar{t}$ CROSS-SECTION MEASUREMENTS IN THE LEPTON+JETS CHANNEL AT $\sqrt{s} = 13$ TeV USING THE ATLAS DETECTOR*

Rafał Bielski

on behalf of the ATLAS Collaboration

University of Manchester, Manchester, United Kingdom

(Received March 21, 2017)

Measurements of differential cross sections of top-quark pair production are presented as a function of the top quark and $t\bar{t}$ system kinematic observables in proton–proton collisions at a centre-of-mass energy of $\sqrt{s} = 13$ TeV. The dataset corresponds to an integrated luminosity of 3.2 fb^{-1}, recorded in 2015 with the ATLAS detector at the CERN Large Hadron Collider. Events with one lepton and jets in the final state are used for the measurement. Two separate selections are applied that each focus on different top-quark momentum phase-spaces, denoted as resolved and boosted topologies of the $t\bar{t}$ final state. The measured spectra are corrected for detector effects and are compared to several Monte Carlo simulations. The results are in a fair agreement with the predictions over a wide kinematic range. Nevertheless, most event generators predict a harder top-quark transverse momentum distribution at high values than what is observed in the data.

DOI:10.5506/APhysPolB.48.921

1. Introduction

Top-quark pair production is one of the key processes allowing for precision measurements of the Standard Model (SM) physics at the TeV scale in proton–proton collisions at the Large Hadron Collider (LHC) at CERN. The large cross section for this process at the centre-of-mass energy of $\sqrt{s} = 13$ TeV provides sufficient statistics for differential measurements in a range of kinematic properties of the top quark and the $t\bar{t}$ system. Such measurements provide a verification of the SM predictions and can also probe physics beyond the SM, which can *e.g.* modify the shape of distributions like the $t\bar{t}$ system mass [1]. Measurements of differential $t\bar{t}$ production cross sections have also been shown to be a valuable input to parton distribution

* Presented at the Cracow Epiphany Conference "Particle Theory Meets the First Data from LHC Run 2", Kraków, Poland, January 9–12, 2017.

function (PDF) fits, able to constrain the gluon PDF at large x [2]. They are also used to validate the Monte Carlo (MC) simulations and tune MC generator settings [3].

The ATLAS experiment [4] at the LHC is a multi-purpose particle detector with a forward–backward symmetric cylindrical geometry and a near to 4π coverage in solid angle[1]. It consists of an inner tracking detector surrounded by a superconducting solenoid providing a 2 T axial magnetic field, electromagnetic (EM) and hadron calorimeters, and a muon spectrometer. The inner tracking detector covers the pseudorapidity range $|\eta| < 2.5$ and consists of silicon pixel, silicon micro-strip, and transition radiation tracking detectors. Lead/liquid-argon (LAr) sampling calorimeters provide EM energy measurements with high granularity. A hadron calorimeter (iron/scintillator-tile) covers the central pseudorapidity range ($|\eta| < 1.7$). The end-cap and forward regions are instrumented with LAr calorimeters for both EM and hadronic energy measurements up to $|\eta| = 4.9$. The Muon Spectrometer (MS) surrounds the calorimeters and is based on three large air-core toroid superconducting magnets with eight coils each. The magnets' bending power ranges from 2.0 to 7.5 Tm. The MS includes a system of precision tracking chambers and fast detectors for triggering.

This article presents a brief overview of the measurement which is comprehensively described in the ATLAS note [5] (a corresponding journal publication is in preparation).

2. Data and simulated samples

The measurement is performed using the dataset collected by the ATLAS detector in 2015 during the LHC pp run at $\sqrt{s} = 13$ TeV with 25 ns bunch spacing. Only data collected with stable beams and good detector status are selected, resulting in a dataset corresponding to an integrated luminosity of 3.2 fb^{-1} $\pm$ 2.1%. The average number of interactions per bunch crossing (pile-up) in the dataset ranges between approximately 5 and 25, with a mean of 14.

The signal and background processes are modelled using MC generators, as listed in [5]. In order to correctly account for the pile-up, each simulated signal or background event is overlaid with multiple proton–proton collisions simulated with the soft QCD processes of PYTHIA 8.186 using the A2

[1] ATLAS uses a right-handed coordinate system with its origin at the nominal interaction point (IP) in the centre of the detector and the z-axis along the beam pipe. The x-axis points from the IP to the centre of the LHC ring, and the y-axis points upwards. Cylindrical coordinates (r, ϕ) are used in the transverse plane, ϕ being the azimuthal angle around the z-axis. The pseudorapidity is defined in terms of the polar angle θ as $\eta = -\ln\tan(\theta/2)$. Angular distance is measured in units of $\Delta R \equiv \sqrt{(\Delta\eta)^2 + (\Delta\phi)^2}$.

tune and the MSTW2008LO PDF set. The samples are then reweighted to match the observed distribution of the number of pp interactions per bunch crossing. The detector response is simulated in Geant 4.

3. Object and event selection

Five types of objects are considered in the measurement: electrons, muons, small- and large-radius anti-k_{T} jets ($R = 0.4$ and 1.0 respectively), and missing transverse momentum $E_{\mathrm{T}}^{\mathrm{miss}}$. All detector-level objects are reconstructed following typical reconstruction algorithms in ATLAS, as detailed in [5]. Particle-level objects are defined for simulated events in analogy to the detector-level objects and constructed from stable final-state particles only. Events are required to contain exactly one lepton (electron or muon) and pass a corresponding single-lepton trigger selection. Two different selections are further defined, aiming at event topologies with different ranges of top-quark momentum. The resolved topology events are required to contain at least four small-R jets, two of which have to be identified as coming from b-quark decays (*b-tagged*). The boosted topology events are required to contain at least one small-R b-tagged jet and at least one large-R jet identified as coming from a top quark with a subsequent hadronic decay of

TABLE I

Summary of the requirements for detector-level and MC-generated particle-level events, for both the resolved and boosted event selections [5].

Level	Detector		Particle
Topology	Resolved	Boosted	
Leptons	$\lvert d_0/\sigma(d_0)\rvert < 5$ and $\lvert z_0 \sin\theta\rvert < 0.5$ mm Track-Calo-based Isolation $\lvert\eta\rvert < 1.37$ or $1.52 < \lvert\eta\rvert < 2.47$ (e), $\lvert\eta\rvert < 2.5$ (μ) E_{T} (e), p_{T} (μ)> 25 GeV		$\lvert\eta\rvert < 2.5$ $p_{\mathrm{T}} > 25$ GeV
Small-R jets	$\lvert\eta\rvert < 2.5$ $p_{\mathrm{T}} > 25$ GeV JVT cut (if $p_{\mathrm{T}} < 60$ GeV and $\lvert\eta\rvert < 2.4$)		$\lvert\eta\rvert < 2.5$ $p_{\mathrm{T}} > 25$ GeV
No. of small-R jets	≥ 4 jets	≥ 1 jet	the same as detector level
$E_{\mathrm{T}}^{\mathrm{miss}}$, m_{T}^{W}	no requirements	$E_{\mathrm{T}}^{\mathrm{miss}}$> 20 GeV, $E_{\mathrm{T}}^{\mathrm{miss}} + m_{\mathrm{T}}^{W} > 60$ GeV	the same as detector level
Leptonic top	kinematic reconstruction	at least one small-R jet with $\Delta R(\ell$, small-R jet$) < 2.0$	kinematic reconstruction
Hadronic top	kinematic reconstruction	the leading-p_{T} trimmed large-R jet has: $\lvert\eta\rvert < 2.0$ 300 GeV $< p_{\mathrm{T}} <$ 1500 GeV, $m > 50$ GeV, Top-tagging at 80% efficiency ΔR(large-R jet, small-R jet) > 1.5, $\Delta\phi(\ell$, small-R jet$) > 1.0$	**Resolved:** kinematic reconstruction **Boosted:** $\lvert\eta\rvert < 2.0$ $300 < p_{\mathrm{T}} < 1500$ GeV Top-tagging: $m > 100$ GeV, $\tau_{32} < 0.75$
b-tagging	at least 2 b-tagged jets	at least one of: (1) the leading-p_{T} small-R jet with $\Delta R(\ell$, small-R jet$) < 2.0$ is b-tagged (2) at least one small-R jet with ΔR(large-R jet, small-R jet) < 1.0 is b-tagged	ghost-matched B-hadron

the W boson (*top-tagged*). Such top quarks are referred to as *hadronic top*, whereas *leptonic top* is analogically defined as a top quark with a subsequent leptonic W decay. In the boosted selection, the highest transverse momentum top-tagged large-R jet is directly used as a proxy of the hadronic top, whereas in the resolved selection, a kinematic reconstruction of both top quarks is performed using the pseudo-top algorithm [6]. The detailed object and event selection is summarised in Table I.

4. Background estimation

Events from other processes than top-quark pair production may also satisfy the event selections described above. These include single top-quark production, W or Z boson production in association with additional jets, diboson production, $t\bar{t}$ production in association with a W or Z boson, and multi-jet events with a fake or non-prompt lepton. The single top, Z+jets, diboson and $t\bar{t}W/t\bar{t}Z$ contribution in the measured distributions is estimated using only MC simulations normalised to higher-order inclusive cross section. The W+jets background estimate uses simulated distribution shapes with data-driven normalisation factor, as well as data-driven scale factors correcting the flavour composition of the additional jets. The multi-jet background is estimated using the data-driven matrix method [7], based on efficiencies to select events with a real or fake lepton which are measured in data control regions. The sum of background contributions in each measured observable is subtracted prior to the unfolding procedure described in the next section.

5. Observables and unfolding procedure

The $t\bar{t}$ production cross section is measured as a function of seven variables: transverse momentum and rapidity of the hadronic top in both, resolved and boosted selections, as well as the transverse momentum, rapidity and mass of the $t\bar{t}$ system in the resolved selection. The differential production cross section in the $i^{\rm th}$ bin of the variable X is calculated as

$$\frac{\mathrm{d}\sigma^{\rm fid}}{\mathrm{d}X^i} \equiv \frac{1}{\mathcal{L}\,\Delta X^i}\,\frac{1}{\epsilon^i}\sum_j \mathcal{M}^{-1}_{ij}\,f^j_{\rm match}\,f^j_{\rm acc}\left(N^j_{\rm reco}-N^j_{\rm bg}\right), \tag{1}$$

where the index j iterates over bins of X at detector level and the index i labels the particle-level bins of X. The procedure starts with subtracting the estimated background yield $N^j_{\rm bg}$ from the observed detector-level data yield $N^j_{\rm reco}$. The resulting number is then multiplied by the acceptance correction factor, $f^j_{\rm acc}$, correcting for the number of events which are generated outside the fiducial phase-space but pass the detector-level selection. In the resolved selection, only events with a good angular correspondence between the particle and detector-level objects are considered. The fraction of rejected events is corrected for by introducing the matching efficiency f^{j}_{match}. Such background-subtracted and corrected detector-level event yields are an input to an iterative Bayesian unfolding procedure (as implemented in RooUnfold), symbolised by $\mathcal{M}^{-1}_{ij}$ and using the migration matrix $\mathcal{M}$ which is mapping the binned generated particle-level events to the binned detector level events. The unfolded spectrum is divided by the reconstruction efficiency ϵ^{i} which corrects for events passing the particle-level selection but not reconstructed at the detector level, and divided by the bin width ΔX^{i} and the integrated luminosity $\mathcal{L}$. The integrated (over the kinematic bins) unfolded cross section σ^{fid} is used to compute the normalised differential cross section $1/\sigma^{\mathrm{fid}}\,\mathrm{d}\sigma^{\mathrm{fid}}/\mathrm{d}X^{i}$.

6. Uncertainties

To evaluate the impact of each uncertainty after the unfolding, the reconstructed distribution in simulation is varied, unfolded using corrections from the nominal POWHEG-BOX signal sample and the unfolded varied distribution is compared to the known particle-level distribution. All detector- and background-related systematic uncertainties are evaluated using the same generator, while alternative generators are employed to assess modelling systematic uncertainties. In these cases, the corrections, derived from one generator, are used to unfold the detector-level spectra of the alternative generator. A detailed description of the uncertainty evaluation procedures is presented in [5]. The leading uncertainties limiting the measurement precision come from small-R jet energy scale and resolution, large-R jet mass scale and energy resolution, the b-tagging efficiency, signal modelling and background estimation.

7. Results and conclusions

Absolute and normalised differential cross-section measurements in all seven variables are presented in [5]. The normalised differential cross section as a function of hadronically decaying top-quark transverse momentum are shown in Fig. 1. The resolved selection measurements present a precision of 10–15% for the absolute spectra and 5–10% for the relative in most bins, whereas the precision in the boosted selection varies between 20% and approximately 50%. The results show a good agreement between the predictions and data in a wide kinematic region. However, the hadronic top p_{T} distribution tends to be harder in all NLO+PS predictions than what is observed in data, for both selections. This tendency has been also observed by the ATLAS and CMS collaborations in previous measurements at lower pp collision energy.

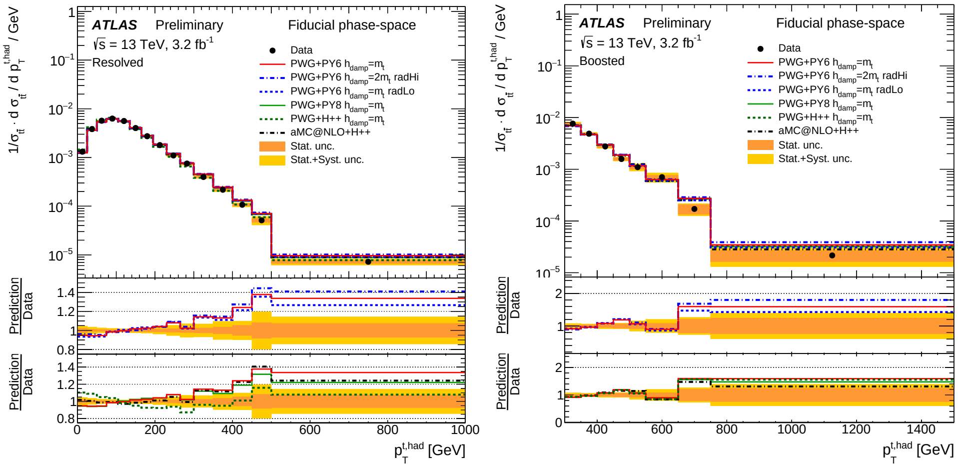

Fig. 1. Normalised differential $t\bar{t}$ production cross sections as a function of hadronic top transverse momentum in the resolved (left) and boosted (right) selections [5].

REFERENCES

- [1] R. Frederix, F. Maltoni, *J. High Energy Phys.* **0901**, 047 (2009) [arXiv:0712.2355 [hep-ph]].
- [2] M. Czakon *et al.*, *J. High Energy Phys.* **1704**, 044 (2017) [arXiv:1611.08609 [hep-ph]].
- [3] ATLAS Collaboration, ATL-PHYS-PUB-2016-020, http://cds.cern.ch/record/2216168
- [4] ATLAS Collaboration, *JINST* **3**, S08003 (2008).
- [5] ATLAS Collaboration, ATLAS-CONF-2016-040, http://cdsweb.cern.ch/record/2206075
- [6] ATLAS Collaboration, *J. High Energy Phys.* **1506**, 100 (2015).
- [7] ATLAS Collaboration, *Phys. Lett. B* **711**, 244 (2012).